

Direct Air Capture of CO₂ Using a Liquid Amine–Solid Carbamic Acid Phase-Separation System Using Diamines Bearing an Aminocyclohexyl Group

Soichi Kikkawa, Kazushi Amamoto, Yu Fujiki, Jun Hirayama, Gen Kato, Hiroki Miura, Tetsuya Shishido, and Seiji Yamazoe*



Cite This: <https://doi.org/10.1021/acsenvironau.1c00065>



Read Online

ACCESS |

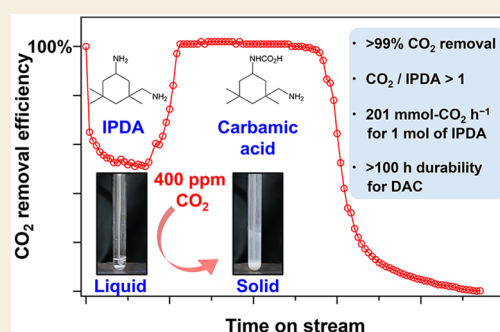
Metrics & More

Article Recommendations

Supporting Information

ABSTRACT: The phase separation between a liquid amine and the solid carbamic acid exhibited >99% CO₂ removal efficiency under a 400 ppm CO₂ flow system using diamines bearing an aminocyclohexyl group. Among them, isophorone diamine [IPDA; 3-(aminomethyl)-3,5,5-trimethylcyclohexylamine] exhibited the highest CO₂ removal efficiency. IPDA reacted with CO₂ in a CO₂/IPDA molar ratio of ≥ 1 even in H₂O as a solvent. The captured CO₂ was completely desorbed at 333 K because the dissolved carbamate ion releases CO₂ at low temperatures. The reusability of IPDA under CO₂ adsorption-and-desorption cycles without degradation, the >99% efficiency kept for 100 h under direct air capture conditions, and the high CO₂ capture rate (201 mmol/h for 1 mol of amine) suggest that the phase separation system using IPDA is robust and durable for practical use.

KEYWORDS: direct air capture, amine method, aqueous amine sorbent, phase change sorbent, carbamic acid, isophoron diamine, aminocyclohexyl group



1. INTRODUCTION

Reducing the concentration of carbon dioxide (CO₂) in the atmosphere is becoming essential for building a sustainable society because an increase in the atmospheric concentration of CO₂ is closely linked to global warming and climate change.¹ Reduction of atmospheric CO₂ levels will require a concerted effort to both limit future emissions of CO₂ and to implement strategies for decreasing the existing atmospheric concentration of CO₂. Artificial storage of CO₂ through direct injection into underground strata or the oceans is relatively well established and has attained plant-level operation;^{2,3} however, such carbon capture and storage techniques involve the risk of subsequent CO₂ leakage. On the other hand, the utilization of CO₂ as a value-added product by carbon capture and storage (CCS) is expected to provide a potential strategy for maintaining net CO₂ emissions at zero.^{4–7} However, the existing CCS technology requires further development to improve the CO₂ absorption/desorption efficiency of sorbents and to establish methods for subsequent conversion of captured CO₂.

Among CCS techniques, the use of sorbents for directly capturing CO₂ (<500 ppm) from the air, known as direct air capture (DAC), is a promising technology and desired to operate under a flow of ambient or low-pressure compressed gas.^{7–9} The challenge in the sorbents for DAC techniques is the high absorption efficiency of low-concentration CO₂

because the existing CCS techniques have insufficient absorption efficiency to perfectly remove the low-concentration CO₂. In addition, the CO₂-desorption temperature from the sorbent should be reduced; currently, the most-well-established sorbent, 2-aminoethanol (monoethanolamine; MEA), requires a temperature of >393 K for efficient CO₂ desorption.^{6,10–12} Finally, the reusability and durability of the sorbents for use in CO₂ capture-and-desorption cycles are required to reduce the frequency of their regeneration and/or replacement. An ideal sorbent should be easily separated and collected from the absorption apparatus for subsequent regeneration.

To satisfy these demands, a number of solid amine-based sorbents^{13–22} and CO₂-absorption systems that utilize phase separation^{23–33} have been developed. The ability of homogeneous liquid-phase systems to absorb CO₂ has been improved by modifying the structures of the amine sorbents. Hanusch *et al.* discovered that pyrrolizidine-based diamines showed a more-efficient CO₂ capture than conventional MEA (Figure

Received: December 29, 2021

Revised: April 27, 2022

Accepted: April 28, 2022

1A-a).³⁴ Although these are promising sorbents for CO₂ capture and desorption, further improvements in the rate of

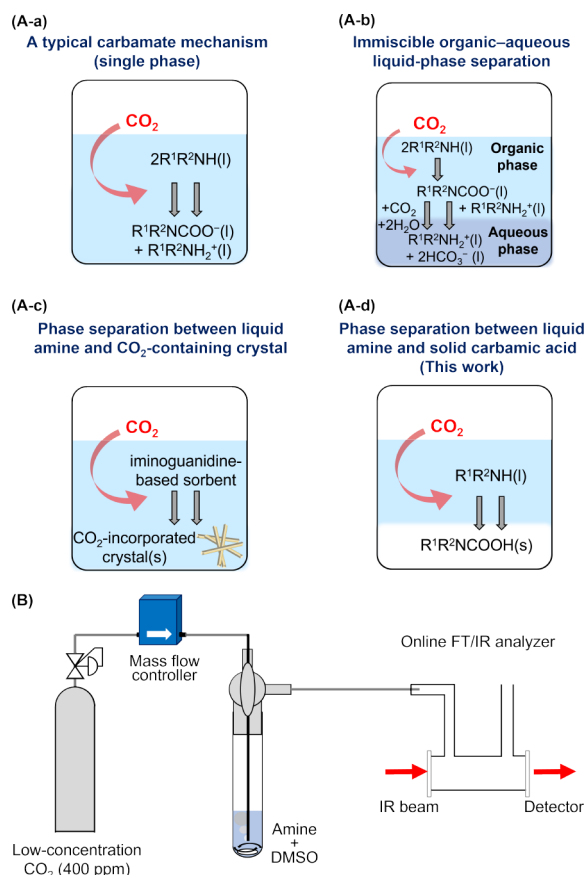


Figure 1. (A) CO₂ absorption/desorption system using phase separation. (a) Typical carbamate mechanism (ref 37). (b) Liquid–liquid phase-change solvents (ref 27). (c) Liquid–solid phase separation with an iminoguanidine-based sorbent (refs 23 and 24). (d) Liquid–solid phase separation with solid carbamate acid formation (this work). (B) Ambient-flow-type reactor equipped with an online FT/IR analyzer for a direct air capture system.

CO₂ absorption and a more efficient absorption at low CO₂ concentrations are required. Liquid–liquid phase separation of amine–H₂O mixtures with lower critical solution temperatures has recently been developed to reduce the costs of regenerating the sorbent (Figure 1A-b).^{27,35,36} After CO₂ absorption, the organic and aqueous phases in these phase-change systems are immiscible, of which the CO₂-rich aqueous phases are suitable to concentrate CO₂ by heating.²⁷ Such systems have achieved higher CO₂ capacities and lower costs compared with those of conventional MEA sorbent-based systems.³⁵ However, the solvents used in the phase-change systems are volatile and corrosive, limiting their range of operating conditions. Actually, the abovementioned systems were evaluated in static systems under ambient or high-pressure CO₂. To establish an efficient system under a flow of low-concentration CO₂, new concepts for sorbents are required.

According to the proposed carbamate mechanism of MEA [$2R^1R^2NH_2(l) + CO_2(g) \rightarrow R^1R^2NH-COO^-(l) + R^1R^2NH_3^+(l)$], the produced carbamate ion inhibits the forward reaction.³⁷ Liquid–solid phase separation provides a possible way of overcoming the equilibrium limitations that inhibit the efficient CO₂ absorption. If the products from the

absorption of CO₂ are solids, their equilibrium concentration in the liquid phase will remain low, thus leading to a high absorption rate of CO₂ into the liquid phase. Moreover, as another benefit, liquid sorbents contact dissolved CO₂ much more efficiently than solid sorbents, which allows efficient absorption of low-concentration CO₂ from large-scale gas streams. The same liquid–solid phase separation systems have been reported up to now under high-concentration CO₂ conditions using triethylenetetramine with polyethylene glycol,²⁵ bis(iminoguanidine),^{23,24,26,28,30} and potassium prolinate.³¹ Custelcean *et al.* recently developed a DAC system using liquid–solid phase separation over an amino acid potassium solution followed by the reaction with a guanidine compound, resulting in the crystallization of insoluble carbonate salt (Figure 1A-c).^{23,24} These systems could remove CO₂ from the air, but they require a sequential CO₂ transfer system. In another iminoguanidine-based sorbent reported by Cai *et al.*, CO₂ desorption from the CO₂-incorporated crystal began at 333 K, and complete CO₂ release required high temperatures above 393 K.²⁹ In addition, this system requires a large amount of solvent because of the low solubility of the sorbent. Further research is therefore required to develop a versatile and simple solid–liquid separation system that are suitable for ambient CO₂ absorption and that lead to efficient CO₂ desorption at low temperatures.

Here, we focus on carbamic acids that exist as a minor-route intermediates [$R^1R^2NH_2(l) + CO_2(g) \rightarrow R^1R^2NH-COOH(l)$].^{37,38} Especially, the carbamic acids that have low solubility compared with corresponding liquid amines are promising to solidification. If a liquid amine forms a solid carbamic acid by reaction with CO₂ [$R^1R^2NH_2(l) + CO_2(g) \rightarrow R^1R^2NH-COOH(s)$], an efficient CO₂ absorption system might be established due to the liquid–solid phase separation and the high amine-utilization efficiency (a 1:1 CO₂-to-amine ratio) (Figure 1A-d). Inagaki *et al.* reported that an aqueous solution of alkylamines with a hydrophobic phenyl group, such as 1,3-phenylenedimethanamine and phenylmethanamine, exhibited absorption capacity with high selective CO₂ absorption from an enclosed ambient air, accompanied with the formation of insoluble carbamic acid.³⁹ This liquid–solid phase change with carbamic acid formation has potential for a high absorption rate of CO₂ at a low CO₂ concentration even under a flow system. Furthermore, in the desorption system under heating, the increase in the solubility of solid carbamic acids would aid the efficient desorption of CO₂.

In this study, we investigated a number of amine compounds to verify our hypothesis by comparison with a conventional amine absorption system using MEA, which works under high CO₂ concentration conditions,³⁷ and KOH aqueous solution, which is applied for the DAC system.⁴⁰ First, we evaluated their CO₂ removal efficiency in a flow system under a low-concentration CO₂ (Figure 1B). We found that diamines with an aminocyclohexyl group showed a high CO₂ removal efficiency as liquid–solid phase-separation sorbents. In particular, isophorone diamine [IPDA; 3-(aminomethyl)-3,5,5-trimethylcyclohexylamine] exhibited a superior CO₂ absorption efficiency under a wide range of CO₂ concentrations (400 ppm to 30%) in a N₂ stream, with solidification of the corresponding carbamic acid. The highly efficient CO₂ removal liquid–solid phase-separation phenomenon was observed in various solvents including H₂O. Moreover, this carbamic acid discharged CO₂ at a lower temperature than a conventional MEA-based system and it exhibited remarkable

reusability. This benchmark study is the first demonstration of a potential DAC system with >90% CO₂ removal efficiency and reusability that is based on the phase separation between a liquid amine sorbent and a solid carbamic acid.

2. RESULTS AND DISCUSSION

Figure 2A shows the efficiency of removal of 400 ppm CO₂ from a flowing CO₂–N₂ mixture for amine-based sorbents in

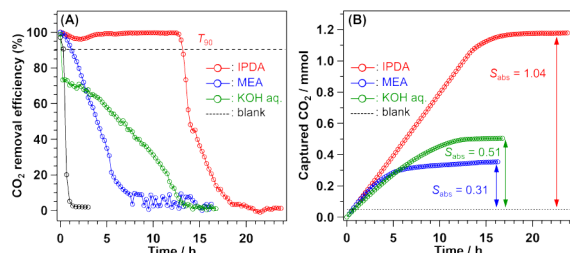


Figure 2. (A) CO₂ removal efficiency over IPDA (red circles) and MEA (blue circles) in DMSO and aqueous solution of 1 M KOH (green circles). Black circles represent the downstream CO₂ concentration w/o sorbents in DMSO. (B) Total amounts of captured CO₂ over IPDA (red circles) and MEA (blue circles) in DMSO and aqueous solution of 1 M KOH (green circles). The dashed line represents the amount of captured CO₂ in DMSO. Reaction conditions: 400 ppm CO₂–N₂ at a flow rate of 75 mL min^{−1}. Amines: 1 mmol, DMSO: 1 mL. KOH: 1 mmol, H₂O: 1 mL.

dimethyl sulfoxide (DMSO) solution. IPDA maintained almost 100% efficiency (CO₂ absorption rate: 80 mmol h^{−1} for 1 mol of amine) for CO₂ removal over 13 h; its efficiency then suddenly decreased, reaching 0% after 21 h. We defined the duration above >90% efficiency as *T*₉₀, and IPDA showed *T*₉₀ of 13 h. The total amount of captured CO₂ (*S*_{abs}) by IPDA reached 1.04 mmol (Figure 2B and Table S1). Figure 3 and

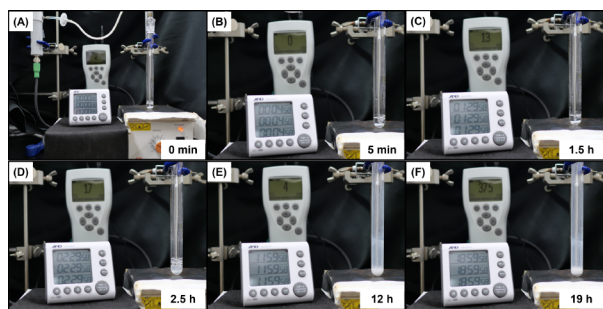
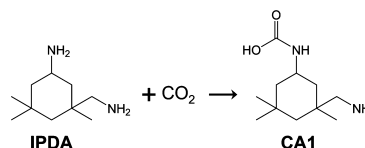


Figure 3. Photographs of a DMSO solution of IPDA under a 400 ppm CO₂–N₂ flow. (A) 0 min, (B) 5 min, (C) 1.5 h, (D) 2.5 h, (E) 12 h, and (F) 19 h. The downstream concentration CO₂ was monitored by using a nondispersive infrared CO₂ meter (GMP252, Vaisala GmbH).

Supporting Video S1 show the changes that occurred during the CO₂ absorption process of Figure 2. A white solid formed after a reaction time of 2.5 h, and the viscosity of IPDA solution gradually increased as the precipitate formed. MEA, a typical amine-based sorbent, showed a lower efficiency of CO₂ removal than IPDA under the same conditions (Figure 2A). After 10 h, the removal efficiency of MEA reached 0% with an *S*_{abs} of 0.31 mmol. The low CO₂ removal efficiency was also obtained for the 1 M KOH aqueous solution, which is applied for the DAC system, as shown in Figure 2A,B.

The solid precipitate was analyzed by FT-IR and ¹³C and ¹H NMR. The FT-IR spectrum of the precipitate (Figure S1) showed the absorption bands at 1600–1660 and 1500–1600 cm^{−1}, assigned to the carboxyl (–COOH) and amido groups (–NH–CO–), respectively, which are characteristics of carbamic acid.⁴¹ In addition, the absorption bands (3165, 3277, and 3346 cm^{−1}), which are characteristics of amine connected with the cyclohexyl group, disappeared, although the absorption bands of another amino group (the shoulder peak in Figure S1B at 1600 cm^{−1} and the broad peak in Figure S1C at 3200–3400 cm^{−1}) remained in the precipitate. ¹³C NMR spectroscopy also indicated that the carbonyl species were incorporated into the precipitate (Figure S2). ¹H NMR spectra showed a larger shift of the peak ascribed to a proton at the secondary carbon bearing an amino group than that ascribed to a proton at the primary aminomethyl group (Figure S3), which enables us to understand that CO₂ preferentially bound to only –NH₂ connected with a cyclohexyl group. From the reaction ratio of IPDA:CO₂ = 1:1 and FT-IR and ¹³C and ¹H NMR analyses, we concluded that the carbamic acid ([3-(aminomethyl)-3,5,5-trimethylcyclohexyl]carbamic acid, CA1) was formed by the following reaction (Scheme 1);

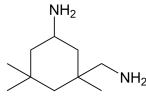
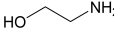
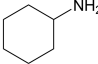
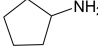
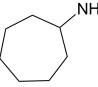
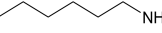
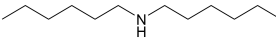
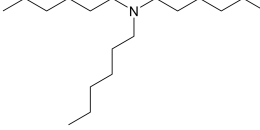
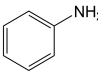
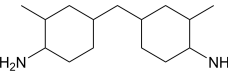
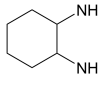
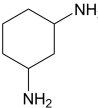
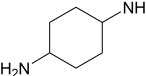
Scheme 1. Formation of CA1 from IPDA



IPDA also showed higher CO₂ removal efficiencies even under the 1% and 30% CO₂ conditions than MEA, as shown in Figure S4. In the case of 30% CO₂, the CO₂ removal efficiency over IPDA remained above 90% over 24 min with an *S*_{abs} of 6.21 mmol. MEA showed a slightly lower durability and capacity (*S*_{abs} = 4.46 mmol). The *S*_{abs}/amine molecule ratios (*R*_{CO₂/molecule}) for IPDA hardly depended on the CO₂ concentration, whereas those for MEA drastically decreased when using a low-concentration CO₂ (Table S1). Thus, IPDA is a superior sorbent to MEA over a wide range of CO₂ concentrations.

Next, the amine scope has been carried out to determine the suitable amine compound for this liquid–solid phase-separation system. Table 1 and Figure S5 summarize the CO₂-absorption capacities of various amines under a 1% CO₂–N₂ flow. IPDA exhibited a superior CO₂ absorption durability even to that of equimolar-amine-containing MEA (Table 1, entries 1–3). The *R*_{CO₂/molecule} for cycloalkyl amines (entries 4–6) was <0.6, which was *ca.* half of that of IPDA (entry 1). In addition, the *T*₉₀ of these amines (entries 4–6) were shorter than that of IPDA (entry 1). Primary amines showed superior amine efficiencies to those of secondary and tertiary amines, probably due to steric hindrance (entries 7–9). In addition, aniline, in which the primary amine group is attached to a phenyl group, absorbed hardly any CO₂ (entry 10). Cycloalkyl diamines (entries 1 and 11–14) formed precipitates and showed relatively high *T*₉₀ values. The diamines bearing an aminocyclohexyl group investigated in this study showed *R*_{CO₂/molecule} ≈ 1.0, indicating that the one –NH₂ connected with a cyclohexyl group in diamines preferentially reacted with CO₂. In addition, IPDA exhibited a CO₂-removal efficiency over a long time (*T*₉₀ = 121 min). Among the regioisomeric

Table 1. CO₂ Absorption Capacities of Various Amines^a

| Entry | Amine | Precipitate | <i>T</i> ₉₀ / min | <i>R</i> _{CO2} /molecule |
|-------|--|------------------|------------------------------|-----------------------------------|
| 1 | IPDA  | formed | 121 | 1.08 |
| 2 | MEA  | n.d. | 43 | 0.62 |
| 3 | MEA ^b | n.d. | 68 | 0.60 |
| 4 | cyclohexylamine  | n.d. | 27 | 0.56 |
| 5 | cyclopentylamine  | n.d. | 23 | 0.49 |
| 6 | cycloheptylamine  | n.d. | 28 | 0.53 |
| 7 | hexylamine  | n.d. | 55 | 0.76 |
| 8 | dihexylamine  | n.d. | 9 | 0.23 |
| 9 | trihexylamine  | n.d. | 6 | n.d. |
| 10 | aniline  | n.d. | 2 | n.d. |
| 11 | 4,4'-methylenebis-(2-methylcyclohexylamine)  | formed | 61 | 1.02 |
| 12 | cyclohexane-1,2-diamine  | partially formed | 36 | 0.92 |
| 13 | cyclohexane-1,3-diamine  | formed | 104 | 1.04 |
| 14 | cyclohexane-1,4-diamine  | formed | 64 | 0.98 |

^aCO₂ absorption capability was evaluated under a 1% CO₂–N₂ flow. Flow rate: 20 mL min^{−1}, amines: 1 mmol, DMSO: 5 mL. ^b2 mmol of MEA was applied, which contains equimolar of amino groups to 1 mmol of IPDA.

cyclohexyldiamines (entries 12–14), cyclohexane-1,2-diamine, with a low *T*₉₀ value of 36 min, afforded a less-viscous solution. These results show that the polarity of the carbamic acid is also essential for efficient CO₂ removal and that differences in the absorption efficiency arise from the rate of formation and the solubility of precipitates from CO₂-absorption reactions.

The CO₂-desorption properties of CA1 were also investigated. Figure 4A shows the desorption rate of CO₂ at various temperatures. CO₂ desorption was first observed at 303 K.

Further desorption occurred on increasing the temperature, and CO₂ was completely desorbed at 333 K. As desorption occurred, the precipitate gradually vanished. Figure 4B shows the desorption profile of CO₂ at 373 K. CO₂ desorption was finished within 20 min, and the maximum CO₂-desorption rate was 134 μmol min^{−1}. This indicates that the low-concentration CO₂ as an ambient air could be condensed to 6% CO₂.

The reusability of IPDA as a sorbent was also examined (Figure 5). The >90% CO₂-capture efficiency was kept for 120

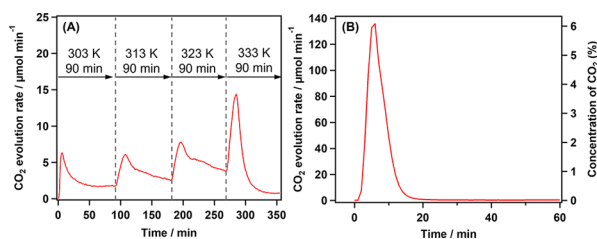


Figure 4. Desorption profile of CO₂ over 1 mmol of CA1 in 15 mL of DMSO under N₂ flow (50 mL min⁻¹). (A) The solution temperature was raised at a range of 303–333 K step by step with a 90 min interval. (B) The solution was heated at 373 K.

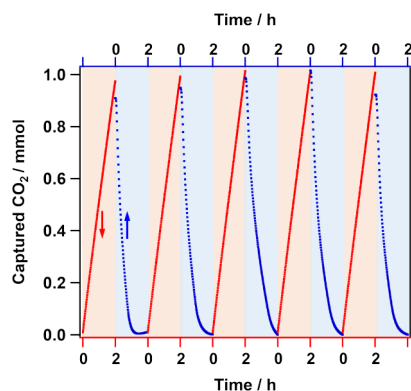


Figure 5. Repetition profile of CO₂ absorption/desorption over 1 mmol of IPDA in 15 mL of DMSO. The absorption capability test under 1% CO₂–N₂ flow (20 mL min⁻¹, 298 K, red line) and desorption of CO₂ under N₂ flow (50 mL min⁻¹, 333 K, blue line) were switched five times with a 120 min interval. The left axis represents the total amounts of captured CO₂.

min, and after switching the gas to N₂ and ramping the temperature to 333 K, the captured CO₂ was perfectly released into the inert gas. The absorption-and-desorption profile is therefore repeatable at least five times without degradation. Note that the desorption temperature was 333 K, which is lower than that for the conventional desorption system with MEA.^{10–12} We therefore consider that IPDA has the potential to replace the existing sorbent in absorption/desorption systems with MEA, which requires a CO₂-desorption temperature of >393 K.

In this study, we found that IPDA efficiently absorbed CO₂ over a wide range of concentrations ranging from 400 ppm to 30% with >90% CO₂ removal efficiency in a flow system and the formation of precipitates of a carbamic acid product. This performance is superior to that of a comparable conventional CO₂-absorption system using MEA. The IPDA-based liquid–solid phase separation system has two advantages. The first is its high $R_{\text{CO}_2/\text{molecule}}$ ratio. The $R_{\text{CO}_2/\text{molecule}}$ ratio for a typical CO₂-absorption system involving a carbamate mechanism is about 0.5 [$2\text{R}^1\text{R}^2\text{NH} + \text{CO}_2 \leftrightarrow \text{R}^1\text{R}^2\text{NCOO}^- \cdots \text{R}^1\text{R}^2\text{NH}_2^+$],³⁷ whereas the $R_{\text{CO}_2/\text{molecule}}$ ratio for the IPDA-based carbamic acid system was near 1.0 [$\text{NH}_2\text{--R--C}_6\text{H}_4\text{--NH}_2(\text{l}) + \text{CO}_2(\text{g}) \rightarrow \text{NH}_2\text{--R--C}_6\text{H}_4\text{--NH--COOH}(\text{s})$]. The second advantage is the high CO₂ removal efficiency (T_{90} value) of the liquid–solid phase separation system, which is achieved as follows. IPDA reacts with CO₂ to form the corresponding carbamic acid in the liquid phase. Initially, the concentrations of carbamic acid in the solution increase to maintain the equilibrium with the carbamate ion [$\text{NH}_2\text{--R--C}_6\text{H}_4\text{--NH--}$

$\text{COO}^- \cdots \text{NH}_2\text{--R--C}_6\text{H}_4\text{--NH}_3^+(\text{l}) \leftrightarrow \text{NH}_2\text{--R--C}_6\text{H}_4\text{--NH}_2(\text{l}) + \text{NH}_2\text{--R--C}_6\text{H}_4\text{--NH--COOH}(\text{l})$].³⁷ When its concentration is saturated, the carbamic acid precipitates from the solution [$\text{NH}_2\text{--R--C}_6\text{H}_4\text{--NH--COOH}(\text{l}) \leftrightarrow \text{NH}_2\text{--R--C}_6\text{H}_4\text{--NH--COOH}(\text{s})$]. In fact, the white carbamate-acid precipitate formed after a reaction time of 1.5 h, as shown in Figure 3 and Supporting Video 1. In addition, the T_{90} strongly depended on the amine concentration and a highly concentrated solution of IPDA showed a high T_{90} value with a high space velocity (SV; flow rate/volume of solution) of 240 h⁻¹ (see Figure S6A and Table S2). The high CO₂ removal efficiency was also achieved under high IPDA concentration conditions (1 mmol of IPDA/1 mL of DMSO, Figure 2A) at an SV of 4500 h⁻¹. In the case of cyclohexylamine that does not form a carbamic acid precipitate under low concentration conditions, the CO₂ absorption behavior was independent of the amine concentration (DMSO: 5–15 mL, SV = 80–240 h⁻¹), whereas 1 mmol of cyclohexylamine in 1 mL of DMSO showed 90% CO₂ removal efficiency under 1% CO₂ conditions with the formation of precipitate, which was confirmed by ¹³C NMR spectroscopy (Figures S2B and S6B). These results indicate that a high concentration of IPDA favors CO₂ absorption and the maintenance of a high absorption rate due to the ease with which the solution becomes saturated with liquid carbamic acid, resulting in the continuous formation of the carbamic acid precipitate (Figure 6A). The phase-separation system

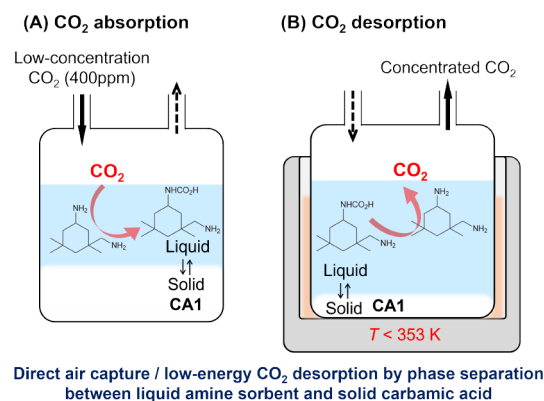


Figure 6. Schematic image of a CO₂ (A) absorption and (B) desorption system using phase separation between liquid IPDA and solid CA1.

therefore overcomes the limitations imposed by the carbamate-ion concentration and the $R_{\text{CO}_2/\text{molecule}}$ ratio. Inagaki *et al.* reported that phenyl group-containing alkylamines, such as 1,3-phenylenedimethanamine and phenylmethanamine, exhibited efficient CO₂ capacity for the DAC system.³⁹ We also tested those amines and found that 1,3-phenylenedimethanamine showed a comparable CO₂ removal efficiency (T_{90}) and CO₂ absorption capacity to IPDA (Figure S7). This diamine formed precipitates when absorbing CO₂, whereas phenylmethanamine maintained the liquid form and showed low CO₂ removal efficiency. We conclude that phase separation between the liquid amine and the solid carbamic acid allows a high amine-utilization efficiency and a high CO₂-removal efficiency compared with the conventional MEA solution, even at ambient CO₂ concentrations.

We also found that CO₂ evolution from the CO₂-absorbed solution containing solid CA1 began to occur at 303 K under a gas flow and that 6% concentration of CO₂ was achieved at

373 K. The thermogravimetry/mass (TG-MS) profile of the solid CA1 showed two steps of weight losses (Figure S8); the first step, which occurred above 333 K, was accompanied with the desorption of CO₂ ($m/z = 44$) and the second step, above 383 K, was attributed to volatilization of IPDA, as its fragmentation patterns appeared in the mass spectrum. Therefore, CA1 should desorb CO₂ without volatilization in the temperature range 333–383 K. However, the desorption of CO₂ from the CO₂-absorbed solution occurred at a lower temperature than that required for solid CA1; the solid CA1 perfectly disappeared by heating at 333 K. This suggests that a part of carbamic acid is dissolved in solution and the carbamic ion, which is formed from carbamic acid in solution, desorbs CO₂ at a low temperature. In addition, the concentration of liquid carbamic acid and carbamate ion increased on heating the solution because the solubility of CA1 increases with increasing temperature (Figure 6B). The liquid–solid phase-separation system is therefore also suitable for the CO₂-desorption process.

Among the diamine-based sorbents tested in this study, IPDA exhibited the best performance that would be related to the solubility and thermal stability of solid carbamic acid (Table S3). Finally, to verify the general versatility of this liquid–solid phase-separation system, the solvent effect on the CO₂ removal efficiency was tested, as shown in Figure S9. The precipitate formed when either DMSO, *N,N*-dimethylformamide (DMF), H₂O, or toluene was used as the solvent at an amine-to-solvent ratio of 1 mmol per 5 mL, whereas the liquid form was maintained for a long time when methanol was used as a solvent, suggesting that the production of precipitate upon CO₂ storage is governed by the solubility of the carbamic acid in each solvent (Table S3). Remarkably, IPDA in H₂O exhibited the highest absorption property (T_{90} and $R_{\text{CO}_2/\text{molecule}}$ ratio) among the solvents, suggesting its practical usefulness. The aqueous IPDA solution showed superior absorption efficiency to MEA with equivalent molar amount (1 mmol MEA), amino groups (2 mmol MEA), and weight (3 mmol MEA) in H₂O solvent and aqueous KOH solution (1 mmol) (Figure 7). In our flow-type system, 5 mmol of KOH (5 M) had a lower removal efficiency than 90% due to the equilibrium (Figure S10). In contrast, the CO₂ absorption rate of aqueous IPDA solution increased after 3 h accompanied with the formation of solid CA1 (Figure 7). After reaching the dissolution limit of liquid carbamic acid, the absorption proceeded accompanied with solid CA1 formation (Figure

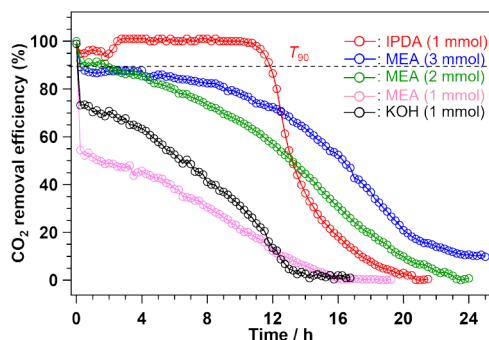


Figure 7. CO₂ removal efficiency over 1 mmol of IPDA (red circles), MEA (3 mmol, blue circles; 2 mmol; green circles, 1 mmol; pink circles), and 1 mmol of KOH (black circles). 400 ppm CO₂–N₂ at a flow rate of 75 mL min^{−1}. H₂O: 1 mL.

S11). Even at high space velocity, the CO₂ absorption rate was enhanced after the CA1 formation, achieving 201 mmol h^{−1} for 1 mol of amine with >90% CO₂ removal efficiency at SV = 11,280 h^{−1} (Figure S12). Moreover, IPDA maintained the >99% removal efficiency of ambient CO₂ from the air for 100 h with the wide-range supply rate of CO₂ (83–114 μmol h^{−1}) (Figure 8). Recently, some efficient amines for DAC, such as

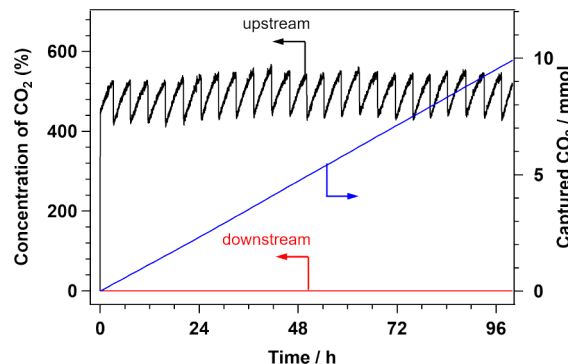


Figure 8. CO₂ concentration at a downstream (red line) and upstream (black line) of the reactor under a compressed ambient air. The total amount of absorbed CO₂ is presented in the right axis. IPDA: 20 mmol, H₂O: 50 mL, gas flow rate: 75 mL min^{−1}. The CO₂ concentration was monitored by using a nondispersive infrared CO₂ meter (GMP252, Vaisala GmbH).

1,3-phenylenedimethanamine (CO₂ absorption rate: 32 mmol h^{−1} for 1 mol of amine)³⁹ and pyrrolizidine (CO₂ absorption rate: 5.0 mmol h^{−1} for 1 mol of amine),³⁴ were reported (Table S4). In the DAC system using amino acid potassium and guanidine, the CO₂ absorption rate was reported to be *ca.* 95 mmol h^{−1} for 1 mol of amine.^{24,26} The DAC system using alkaline base solution has been established in a plant-level operation with the CO₂ absorption rates of 13 mmol h^{−1} for 1 mol of KOH⁴⁰ and 16 mmol h^{−1} for 1 mol of NaOH.⁴² However, the CO₂ desorption temperature is 1173 K,^{7,40,43–45} which is extremely higher than the CO₂ desorption temperature of the present system (333 K). Those results suggest that IPDA, which absorbs CO₂ with sufficient rapidity (CO₂ absorption rate: 201 mmol h^{−1} for 1 mol amine, SV: 11280 h^{−1}, Figure S12), might be a potential candidate for use as an amine-based sorbent for low concentrations of CO₂ and should be suitable for use in a DAC system. In addition, the system works well in H₂O solvent. Therefore, the steam-assisted temperature vacuum-swing adsorption technique^{15,46,47} can be applied to our system. Those features realize high CO₂ absorption and desorption abilities, and our study has demonstrated the possibility of practical applications in low-energy DAC and CO₂-desorption systems.

3. CONCLUSIONS

In this study, we have developed a system for capturing CO₂ directly from the air by using the phase separation between a liquid amine and the solid carbamic acid formed through the absorption of CO₂ by the amine. IPDA exhibited a CO₂ removal efficiency superior to that of MEA with the typical carbamate-based mechanism for a wide range of CO₂ concentrations (400 ppm to 30%). Under 400 ppm CO₂, IPDA reacted with CO₂ in the CO₂/IPDA molar ratio of 1 and exhibited >99% CO₂ removal for more than 13 h. The IPDA system began to desorb CO₂ at ≥303 K and CO₂ was

completely desorbed at 333 K under N₂ flow conditions. The CO₂ capture-and-desorption cycle could be repeated at least five times without degradation. Remarkably, IPDA in H₂O as a solvent was applied to capturing CO₂ from the air for 100 h with >99% efficiency. The removal of IPDA-derived carbamic acid from the H₂O solution as solid during CO₂ absorption realizes high CO₂ removal efficiency even at the high flow velocity of 400 ppm CO₂ (space velocity: 11280 h⁻¹ and CO₂ supply rate: 201 mmol h⁻¹ for 1 mol of IPDA). Moreover, the partially dissolved IPDA-derived carbamic acid easily releases CO₂ in the liquid phase at low temperatures during the CO₂ desorption process. This phase separation system between a liquid amine and the solid carbamic acid formed through absorption/desorption of CO₂ was available for other amines, which form solid carbamic acid by CO₂ absorption.

4. EXPERIMENTAL SECTION

4.1. Chemicals

All chemicals were used as received. Isophorone diamine [IPDA, 3-(aminomethyl)-3,5,5-trimethylcyclohexylamine; *cis/trans* mixture, >99.0%], 2-aminoethanol (MEA, monoethanolamine; >99.0%), cyclohexylamine (>99.0%), cycloheptylamine (>97.0%), cyclopentylamine (>98.0%), hexylamine (>99.0%), dihexylamine (>98.0%), trihexylamine (>98.0%), 4,4'-methylenebis(2-methylcyclohexylamine) (*cis/trans* mixture, >99.0%), cyclohexane-1,2-diamine (*cis/trans* mixture, >98.0%), cyclohexane-1,3-diamine (*cis/trans* mixture, >95.0%), cyclohexane-1,4-diamine (*cis/trans* mixture, >97.0%), 1,3-phenylenedimethanamine (>99.0%), phenylmethanamine (>99.0%), *N,N*-dimethylformamide (DMF; >99.0%), and dimethyl sulfoxide (DMSO; >99.0%) were purchased from Tokyo Chemical Industry Co., Ltd. Aniline (>99.0%) and KOH (>85.0%) were purchased from FUJIFILM Wako Pure Chemical Corp. Toluene (>99.5%), methanol (99.8%), and diethyl ether (>99.5%) were purchased from Kanto Chemical Co., Inc.

4.2. CO₂ Absorption

CO₂ absorption was evaluated by using an ambient-flow-type reactor at room temperature (~303 K; uncontrolled) with monitoring by a downstream IR analyzer. Specific proportions of the amine or KOH substrates in DMSO or H₂O were bubbled with a controlled flow of 400 ppm, 1%, or 30% CO₂ in N₂ with vigorous stirring. To suppress the decrease in solvent volume in the reactor due to volatilization, the CO₂-N₂ gas was through into a solvent at an upstream of the reactor. The concentration of CO₂ in an optical cell downstream of the reactor was monitored by using a Fourier-transform infrared spectrometer equipped with a triglycine sulfate detector (FT/IR-4600, JASCO Co. Ltd.; Figure S13). The cell lengths and volumes between the pair of CaF₂ windows were optimized for each gas concentration. Each spectrum was collected from eight scans at a resolution of 4 cm⁻¹. The concentration of CO₂ in the downstream optical cell [*C*_{CO₂}(*t*)] was determined from the area of the absorption peak of CO₂ in the range 2200–2400 cm⁻¹. The amount of CO₂ adsorbed (*S*_{abs}) was calculated by using the following equation:

$$S_{\text{abs}} (\text{mmol}) = S_{\text{app}} - S_{\text{blank}}$$

where *S*_{app} and *S*_{blank} are the apparent amounts of CO₂ adsorbed with and without the amine-based sorbent, respectively. The value of *S*_{app} was calculated as follows:

$$S_{\text{app}} (\text{mmol}) = \int_0^t C_{\text{CO}_2}(t) dt \times F$$

where *F* is the flow rate of the diluted CO₂ gas.

A 4 day long-term durability test was carried out by using 20 mmol of IPDA dissolved in 50 mL of H₂O solvent. Ambient room air compressed by using an oil-free air compressor (Bebicon, HITACHI Co. Ltd.) was supplied at a flow rate of 75 mL min⁻¹. To suppress the decrease in H₂O as a solvent, the humid gas was fed through H₂O

trap. The CO₂ concentrations at up- and downstream of reactor were monitored by using nondispersive infrared CO₂ meters (GMP252, Vaisala GmbH).

4.3. CO₂ Desorption

The desorption of captured CO₂ was evaluated by using the same flow reactor. After storing 1% CO₂-N₂, the gas flow was switched to pure N₂ (50 mL min⁻¹) while the temperature was ramped up to the operating temperature. The reactor temperature rapidly reached the set value within a few minutes. The solution temperature was raised in the range 303–333 K in a stepwise manner with 90 min intervals. The concentration of CO₂ was monitored by using the same IR analyzer as discussed above. For the repeated CO₂ absorption/desorption cycles, a 1% CO₂-N₂ flow at 298 K and a pure N₂ flow at 333 K were switched five times at 120 min intervals.

4.4. Analysis

The CO₂ desorption profile of the obtained solid material was measured by using a thermogravimetric analyzer (STA-2500 Regulus, Netzsch) equipped with a mass spectrometer (JMS-Q1500GC, JEOL). The temperature of the sample holder was ramped to 773 K at a rate of 10 K min⁻¹ under flowing He. The sample was prepared by exposure of IPDA to CO₂ in diethyl ether. The precipitate was collected by centrifugation from diethyl ether, dried at room temperature, and subjected to analysis. Fourier-transform 100 MHz ¹³C NMR spectra were recorded on a JMN-ECS400 instrument (JEOL). Chemical shifts (δ) of the ¹³C{¹H} NMR spectra were referenced to SiMe₄. The samples were prepared by exposing the relevant amines to CO₂ in toluene. Fourier-transform infrared spectra were recorded by a FT/IR-4X (JASCO) equipped with an attenuated total reflection unit.

■ ASSOCIATED CONTENT

Supporting Information

The Supporting Information is available free of charge at <https://pubs.acs.org/doi/10.1021/acsenvironau.1c00065>.

Supporting Video showing the solid formation during CO₂ absorption (MP4)

Performances of reported CO₂ sorbents, ¹³C and ¹H NMR spectra and TG-DTA-MS profile of solid carbamic acid, and photograph of experimental setup (PDF)

■ AUTHOR INFORMATION

Corresponding Author

Seiji Yamazoe – Department of Chemistry, Graduate School of Science, Tokyo Metropolitan University, Hachioji, Tokyo 192–0397, Japan; Elements Strategy Initiative for Catalysts & Batteries (ESICB), Kyoto University, Nishikyō-ku, Kyoto 615–8245, Japan; Research Center for Hydrogen Energy-Based Society, Tokyo Metropolitan University, Hachioji, Tokyo 192–0397, Japan; Precursory Research for Embryonic Science and Technology (PRESTO), Japan Science and Technology Agency (JST), Kawaguchi, Saitama 332-0012, Japan; orcid.org/0000-0002-8382-8078; Email: yamazoe@tmu.ac.jp

Authors

Soichi Kikkawa – Department of Chemistry, Graduate School of Science, Tokyo Metropolitan University, Hachioji, Tokyo 192–0397, Japan; Elements Strategy Initiative for Catalysts & Batteries (ESICB), Kyoto University, Nishikyō-ku, Kyoto 615–8245, Japan; orcid.org/0000-0002-8193-6374

Kazushi Amamoto – Department of Chemistry, Graduate School of Science, Tokyo Metropolitan University, Hachioji, Tokyo 192–0397, Japan

Yu Fujiki – Department of Chemistry, Graduate School of Science, Tokyo Metropolitan University, Hachioji, Tokyo 192–0397, Japan

Jun Hirayama – Department of Chemistry, Graduate School of Science, Tokyo Metropolitan University, Hachioji, Tokyo 192–0397, Japan; Elements Strategy Initiative for Catalysts & Batteries (ESICB), Kyoto University, Nishikyo-ku, Kyoto 615–8245, Japan

Gen Kato – Department of Applied Chemistry for Environment, Graduate School of Urban Environmental Sciences, Tokyo Metropolitan University, Hachioji, Tokyo 192–0397, Japan

Hiroki Miura – Elements Strategy Initiative for Catalysts & Batteries (ESICB), Kyoto University, Nishikyo-ku, Kyoto 615–8245, Japan; Research Center for Hydrogen Energy-Based Society, Tokyo Metropolitan University, Hachioji, Tokyo 192–0397, Japan; Department of Applied Chemistry for Environment, Graduate School of Urban Environmental Sciences, Tokyo Metropolitan University, Hachioji, Tokyo 192–0397, Japan; orcid.org/0000-0002-2488-4432

Tetsuya Shishido – Elements Strategy Initiative for Catalysts & Batteries (ESICB), Kyoto University, Nishikyo-ku, Kyoto 615–8245, Japan; Research Center for Hydrogen Energy-Based Society, Tokyo Metropolitan University, Hachioji, Tokyo 192–0397, Japan; Department of Applied Chemistry for Environment, Graduate School of Urban Environmental Sciences, Tokyo Metropolitan University, Hachioji, Tokyo 192–0397, Japan; orcid.org/0000-0002-8475-4226

Complete contact information is available at:

<https://pubs.acs.org/10.1021/acsenvironau.1c00065>

Author Contributions

S.K. and S.Y. designed this study. K.A. and Y.F. contributed to all experimental works and data analysis. S.K. and J.H. conducted the experimental setup and data analysis. G.K., H.M., and T.S. characterized the carbamic acids. S.K. and S.Y. proposed the mechanism with the help of H.M. and T.S. S.Y. supervised this study. All authors took part in the writing of this manuscript.

Notes

The authors declare no competing financial interest.

ACKNOWLEDGMENTS

This study is based on results obtained from a project, P14004, subsidized by the New Energy and Industrial Technology Development Organization (NEDO).

REFERENCES

- (1) Pachauri, R. K.; Allen, M. R.; Barros, V. R.; Broome, J.; Cramer, W.; Christ, R.; Church, J. A.; Clarke, L.; Dahe, Q.; Dasgupta, P., *Climate Change 2014: Synthesis Report. Contribution of Working Groups I, II and III to the Fifth Assessment Report of the Intergovernmental Panel on Climate Change*; IPCC, 2014.
- (2) Tanaka, Y.; Sawada, Y.; Tanase, D.; Tanaka, J.; Shiomi, S.; Kasukawa, T. Tomakomai CCS Demonstration Project of Japan, CO₂ Injection in Process. *Energy Proc.* **2017**, *114*, 5836–5846.
- (3) Koytsoumpa, E. I.; Bergins, C.; Kakaras, E. The CO₂ Economy: Review of CO₂ Capture and Reuse Technologies. *Journal Supercrit. Fluids* **2018**, *132*, 3–16.
- (4) Yang, H.; Xu, Z.; Fan, M.; Gupta, R.; Slimane, R. B.; Bland, A. E.; Wright, I. Progress in Carbon Dioxide Separation and Capture: A Review. *J. Environ. Sci.* **2008**, *20*, 14–27.

(5) Mikkelsen, M.; Jørgensen, M.; Krebs, F. C. The Teraton Challenge. A Review of Fixation and Transformation of Carbon Dioxide. *Energy Environ. Sci.* **2010**, *3*, 43–81.

(6) Cuéllar-Franca, R. M.; Azapagic, A. Carbon Capture, Storage and Utilisation Technologies: A Critical Analysis and Comparison of Their Life Cycle Environmental Impacts. *J. CO₂ Util.* **2015**, *9*, 82–102.

(7) Sanz-Perez, E. S.; Murdock, C. R.; Didas, S. A.; Jones, C. W. Direct Capture of CO₂ from Ambient Air. *Chem. Rev.* **2016**, *116*, 11840–11876.

(8) Socolow, R.; Desmond, M.; Aines, R.; Blackstock, J.; Bolland, O.; Kaarsberg, T.; Lewis, N.; Mazzotti, M.; Pfeffer, A.; Sawyer, K. *Direct Air Capture of CO₂ with Chemicals: A Technology Assessment for the APS Panel on Public Affairs*; American Physical Society: 2011.

(9) Goeppert, A.; Czaun, M.; Prakash, G. S.; Olah, G. A. Air as the Renewable Carbon Source of the Future: an Overview of CO₂ Capture from the Atmosphere. *Energy Environ. Sci.* **2012**, *5*, 7833–7853.

(10) Liu, Y.; Fan, W.; Wang, K.; Wang, J. Studies of CO₂ Absorption/Regeneration Performances of Novel Aqueous Monoethanolamine (MEA)-Based Solutions. *J. Cleaner Prod.* **2016**, *112*, 4012–4021.

(11) Luis, P. Use of Monoethanolamine (MEA) for CO₂ Capture in a Global Scenario: Consequences and Alternatives. *Desalination* **2016**, *380*, 93–99.

(12) Wang, M.; Wang, M.; Rao, N.; Li, J.; Li, J. Enhancement of CO₂ Capture Performance of Aqueous MEA by Mixing with [NH₂e-mim][BF₄]. *RSC Adv.* **2018**, *8*, 1987–1992.

(13) Xu, X.; Song, C.; Andresen, J. M.; Miller, B. G.; Scaroni, A. W. Novel Polyethylenimine-Modified Mesoporous Molecular Sieve of MCM-41 Type as High-Capacity Adsorbent for CO₂ Capture. *Energy Fuels* **2002**, *16*, 1463–1469.

(14) Khatri, R. A.; Chuang, S. S. C.; Soong, Y.; Gray, M. Thermal and Chemical Stability of Regenerable Solid Amine Sorbent for CO₂ Capture. *Energy Fuels* **2006**, *20*, 1514–1520.

(15) Li, W.; Choi, S.; Drese, J. H.; Hornbostel, M.; Krishnan, G.; Eisenberger, P. M.; Jones, C. W. Steam-Stripping for Regeneration of Supported Amine-Based CO₂ Adsorbents. *ChemSusChem* **2010**, *3*, 899–903.

(16) Liu, Y.; Ye, Q.; Shen, M.; Shi, J.; Chen, J.; Pan, H.; Shi, Y. Carbon Dioxide Capture by Functionalized Solid Amine Sorbents with Simulated Flue Gas Conditions. *Environ. Sci. Technol.* **2011**, *45*, 5710–5716.

(17) Alkhabbaz, M. A.; Bollini, P.; Foo, G. S.; Sievers, C.; Jones, C. W. Important Roles of Enthalpic and Entropic Contributions to CO₂ Capture from Simulated Flue Gas and Ambient Air Using Mesoporous Silica Grafted Amines. *J. Am. Chem. Soc.* **2014**, *136*, 13170–13173.

(18) Wang, J.; Wang, M.; Li, W.; Qiao, W.; Long, D.; Ling, L. Application of Polyethylenimine-Impregnated Solid Adsorbents for Direct Capture of Low-Concentration CO₂. *AIChE J.* **2015**, *61*, 972–980.

(19) Liu, F.; Chen, S.; Gao, Y. Synthesis of Porous Polymer Based Solid Amine Adsorbent: Effect of Pore Size and Amine Loading on CO₂ Adsorption. *J. Colloid Interface Sci.* **2017**, *506*, 236–244.

(20) Ünveren, E. E.; Monkul, B. Ü.; Sarioğlu, Ş.; Karademir, N.; Alper, E. Solid Amine Sorbents for CO₂ Capture by Chemical Adsorption: A Review. *Petroleum* **2017**, *3*, 37–50.

(21) Min, K.; Choi, W.; Kim, C.; Choi, M. Oxidation-Stable Amine-Containing Adsorbents for Carbon Dioxide Capture. *Nat. Commun.* **2018**, *9*, 726–732.

(22) Chen, Y.; Lin, G.; Chen, S. Preparation of a Solid Amine Microspherical Adsorbent with High CO₂ Adsorption Capacity. *Langmuir* **2020**, *36*, 7715–7723.

(23) Seipp, C. A.; Williams, N. J.; Kidder, M. K.; Custelcean, R. CO₂ Capture from Ambient Air by Crystallization with a Guanidine Sorbent. *Angew. Chem., Int. Ed. Engl.* **2017**, *56*, 1042–1045.

(24) Brethomé, F. M.; Williams, N. J.; Seipp, C. A.; Kidder, M. K.; Custelcean, R. Direct Air Capture of CO₂ via Aqueous-Phase

Absorption and Crystalline-Phase Release Using Concentrated Solar Power. *Nat. Energy* **2018**, 3, 553–559.

(25) Tao, M.; Gao, J.; Zhang, W.; Li, Y.; He, Y.; Shi, Y. A Novel Phase-Changing Nonaqueous Solution for CO₂ Capture with High Capacity, Thermostability, and Regeneration Efficiency. *Ind. Eng. Chem. Res.* **2018**, 57, 9305–9312.

(26) Custelcean, R.; Williams, N. J.; Garrabrant, K. A.; Agullo, P.; Brethomé, F. M.; Martin, H. J.; Kidder, M. K. Direct Air Capture of CO₂ with Aqueous Amino Acids and Solid Bis-iminoguanidines (BIGs). *Ind. Eng. Chem. Res.* **2019**, 58, 23338–23346.

(27) Papadopoulos, A. I.; Tzirakis, F.; Tsivintzelis, I.; Seferlis, P. Phase-Change Solvents and Processes for Postcombustion CO₂ Capture: A Detailed Review. *Ind. Eng. Chem. Res.* **2019**, 58, 5088–5111.

(28) Williams, N. J.; et al. CO₂ Capture via Crystalline Hydrogen-Bonded Bicarbonate Dimers. *Chem* **2019**, 5, 719–730.

(29) Cai, H.; Zhang, X.; Lei, L.; Xiao, C. Direct CO₂ Capture from Air via Crystallization with a Trichelating Iminoguanidine Ligand. *ACS Omega* **2020**, 5, 20428–20437.

(30) Custelcean, R.; Williams, N. J.; Wang, X.; Garrabrant, K. A.; Martin, H. J.; Kidder, M. K.; Ivanov, A. S.; Bryantsev, V. S. Dialing in Direct Air Capture of CO₂ by Crystal Engineering of Bisiminoguanidines. *ChemSusChem* **2020**, 13, 6381–6390.

(31) Li, H.; Guo, H.; Shen, S. Low-Energy-Consumption CO₂ Capture by Liquid–Solid Phase Change Absorption Using Water-Lean Blends of Amino Acid Salts and 2-Alkoxyethanols. *ACS Sustainable Chem. Eng.* **2020**, 8, 12956–12967.

(32) Custelcean, R. Direct Air Capture of CO₂ via Crystal Engineering. *Chem. Sci.* **2021**, 12, 12518–12528.

(33) Custelcean, R. Direct Air Capture with Bis-iminoguanidines: From Discovery to Commercialization. *Chem* **2021**, 7, 2848–2852.

(34) Hanusch, J. M.; Kerschgens, I. P.; Huber, F.; Neuburger, M.; Gademann, K. Pyrrolizidines for Direct Air Capture and CO₂ Conversion. *Chem. Commun.* **2019**, 55, 949–952.

(35) Machida, H.; Ando, R.; Esaki, T.; Yamaguchi, T.; Horioze, H.; Kishimoto, A.; Akiyama, K.; Nishimura, M. Low Temperature Swing Process for CO₂ Absorption-Desorption Using Phase Separation CO₂ Capture Solvent. *Int. J. Greenhouse Gas Control* **2018**, 75, 1–7.

(36) Tran, K. V. B.; Ando, R.; Yamaguchi, T.; Machida, H.; Norinaga, K. Carbon Dioxide Absorption Heat in Liquid–Liquid and Solid–Liquid Phase-Change Solvents Using Continuous Calorimetry. *Ind. Eng. Chem. Res.* **2020**, 59, 3475–3484.

(37) Yamada, H. Amine-Based Capture of CO₂ for Utilization and Storage. *Polym. J.* **2021**, 53, 93–102.

(38) Mitsudo, T.-a.; Hori, Y.; Yamakawa, Y.; Watanabe, Y. Ruthenium Catalyzed Selective Synthesis of Enol Carbamates by Fixation of Carbon Dioxide. *Tetrahedron Lett.* **1987**, 28, 4417–4418.

(39) Inagaki, F.; Matsumoto, C.; Iwata, T.; Mukai, C. CO₂-Selective Absorbents in Air: Reverse Lipid Bilayer Structure Forming Neutral Carbamic Acid in Water Without Hydration. *J. Am. Chem. Soc.* **2017**, 139, 4639–4642.

(40) Keith, D. W.; Holmes, G.; St. Angelo, D.; Heide, K. A Process for Capturing CO₂ from the Atmosphere. *Joule* **2018**, 2, 1573–1594.

(41) Dijkstra, Z. J.; Doornbos, A. R.; Weyten, H.; Ernsting, J. M.; Elsevier, C. J.; Keurentjes, J. T. F. Formation of Carbamic Acid in Organic Solvents and in Supercritical Carbon Dioxide. *J. Supercrit. Fluids* **2007**, 41, 109–114.

(42) McQueen, N.; Gomes, K. V.; McCormick, C.; Blumanthal, K.; Pisciotto, M.; Wilcox, J. A Review of Direct Air Capture (DAC): Scaling up Commercial Technologies and Innovating for the Future. *Prog. Energy* **2021**, 3, 032001–032022.

(43) Holmes, G.; Keith, D. W. An Air-Liquid Contactor for Large-Scale Capture of CO₂ from Air. *Philos. Trans. R. Soc., A* **2012**, 370, 4380–4403.

(44) Derevschikov, V. S.; Veselovskaya, J. V.; Kardash, T. Y.; Trubitsyn, D. A.; Okunev, A. G. Direct CO₂ Capture from Ambient Air Using K₂CO₃/Y₂O₃ Composite Sorbent. *Fuel* **2014**, 127, 212–218.

(45) Ngu, L. H.; Song, J. W.; Hashim, S. S.; Ong, D. E. Lab-Scale Atmospheric CO₂ Absorption for Calcium Carbonate Precipitation in Sand. *Greenhouse Gases: Sci. Technol.* **2019**, 9, 519–528.

(46) Wurzbacher, J. A.; Gebald, C.; Piatkowski, N.; Steinfeld, A. Concurrent Separation of CO₂ and H₂O from Air by a Temperature-Vacuum Swing Adsorption/Desorption Cycle. *Environ. Sci. Technol.* **2012**, 46, 9191–9198.

(47) Zhu, X.; Ge, T.; Yang, F.; Wang, R. Design of Steam-Assisted Temperature Vacuum-Swing Adsorption Processes for Efficient CO₂ Capture from Ambient Air. *Renew. Sustainable Energy Rev.* **2021**, 137, 110651–110662.

Recommended by ACS

A Novel Phase-Changing Nonaqueous Solution for CO₂ Capture with High Capacity, Thermostability, and Regeneration Efficiency

Mengna Tao, Yao Shi, et al.

JUNE 25, 2018

INDUSTRIAL & ENGINEERING CHEMISTRY RESEARCH

READ 

Aminoalkyl-Functionalized Pyridines as High Cyclic Capacity CO₂ Absorbents

Sigvart Evjen, Hanna K. Knuutila, et al.

SEPTEMBER 24, 2019

ENERGY & FUELS

READ 

DBU-Glycerol Solution: A CO₂ Absorbent with High Desorption Ratio and Low Regeneration Energy

Xiaoyan Zhu, Bin Liang, et al.

MAY 26, 2020

ENVIRONMENTAL SCIENCE & TECHNOLOGY

READ 

Characterization of CO₂ Absorption and Carbamate Precipitate in Phase-Change N-Methyl-1,3-diaminopropane/N,N-Dimethylformamide Solvent

Jun Cheng, Kefa Cen, et al.

NOVEMBER 14, 2017

ENERGY & FUELS

READ 

Get More Suggestions >